1-1-2017

A robust free-standing MoS2/ poly(3,4-ethylenedioxythiophene):poly(styrenesulfonate) film for supercapacitor applications

Yu Ge
University of Wollongong, yg711@uowmail.edu.au

Rouhollah Jalili
University of Wollongong, rjalili@uow.edu.au

Caiyun Wang
University of Wollongong, caiyun@uow.edu.au

Tian Zheng
University of Wollongong, tz648@uowmail.edu.au

Yunfeng Chao
University of Wollongong, yc682@uowmail.edu.au

See next page for additional authors

A robust free-standing MoS2/ poly(3,4-ethylenedioxythiophene):poly(styrenesulfonate) film for supercapacitor applications

Abstract

Two-dimensional molybdenum disulfide (MoS2) is a promising energy storage material due to its high surface area and unique electronic structure. Free-standing flexible MoS2-based electrode is of importance for use in flexible energy storage devices, whereas there are limited reports available. In this work we developed a robust hybrid film, MoS2 incorporated with highly conductive poly(3,4-ethylenedioxythiophene):poly(styrenesulfonate). This free-standing film possesses excellent mechanical properties with a fracture strength of 18.0 MPa and a Young's modulus of 2.0 GPa. It can deliver a large volumetric capacitance of 141.4 F cm-3, a high volumetric energy density of 4.9 mWh cm-3, and a capacitance retention rate of 98.6% after 5000 charge/discharge cycles. This film has demonstrated its application in an all-solid-state bendable supercapacitor as well.

Disciplines

Engineering | Physical Sciences and Mathematics

Publication Details

Ge, Y., Jalili, R., Wang, C., Zheng, T., Chao, Y. & Wallace, G. G. (2017). A robust free-standing MoS_2/poly(3,4-ethylenedioxythiophene):poly(styrenesulfonate) film for supercapacitor applications. Electrochimica Acta, 235 348-355.

Authors

Yu Ge, Rouhollah Jalili, Caiyun Wang, Tian Zheng, Yunfeng Chao, and Gordon G. Wallace

A robust free-standing MoS_2/poly(3,4-ethylenedioxythiophene):poly(styrenesulfonate) film for supercapacitor applications

Yu Ge, Rouhollah Jalili, Caiyun Wang*, Tian Zheng, Yunfeng Chao and Gordon G. Wallace*

Intelligent Polymer Research Institute, ARC Centre of Excellence for Electromaterials Science, AIIM Facility, Innovation Campus, University of Wollongong, Wollongong, NSW 2522 Australia.

*** Corresponding authors**

Tel: +61 2 42981426. Fax: +61 2 4298 1499. E-mail: caiyun@uow.edu.au (C.W.).

Tel: +61 2 42213127. Fax: +61 2 4298 1499. E-mail: gwallace@uow.edu.au (G.G.W.).

Abstract

Two-dimensional molybdenum disulfide (MoS_2) is a promising energy storage material due to its high surface area and unique electronic structure. Free-standing flexible MoS_2-based electrode is of importance for use in flexible energy storage devices, whereas there are limited reports available. In this work we developed a robust hybrid film, MoS_2 incorporated with highly conductive poly(3,4-ethylenedioxythiophene):poly(styrenesulfonate). This free-standing film possesses excellent mechanical properties with a fracture strength of 18.0 MPa and a Young's modulus of 2.0 GPa. It can deliver a large volumetric capacitance of 141.4 F cm^{-3}, a high volumetric energy density of 4.9 mWh cm^{-3}, and a capacitance retention rate of 98.6% after 5000 charge/discharge cycles. This film has demonstrated its application in an all-solid-state bendable supercapacitor as well.

Key words: molybdenum disulfide, PEDOT:PSS, free-standing film, supercapacitors, conjugated polymer.

1. Introduction

Flexible/bendable electronic equipments such as roll-up displays and wearable devices are currently under rapid development, which urgently requires the development of flexible energy storage devices to match.[1-3] As an important energy storage device, flexible supercapacitor has attracted attention due to its ease of large-scale production and promising electrochemical properties (*i.e.* large capacitance, high power density and long cycle life).[4, 5] Free-standing, binder-free films are one very important type of flexible electrodes, since they can be easily processed into different shapes and sizes for simplicity of device fabrication. Two-dimensional (2D) graphene or conjugated polymers films have demonstrated this use,[6-9] while the pursuit of new materials with higher performance is still in demand.

Molybdenum disulfide (MoS_2) nanosheet, as a typical inorganic analogue of graphene, has emerged as an excellent material for energy storage applications due to its sheet-like structure providing large surface area for charge storage.[10-12] The centre Mo atom in MoS_2 has a wide range of oxidation state from +2 to +6, offering pseudo-capacitances.[13-15] Moreover, MoS_2 is non-toxic, eco-friendly and of low cost.[16]

Li-intercalation exfoliation method is a widely used method to fabricate single- and few-layer MoS_2 nanosheets. The produced high-concentration MoS_2 nanosheets in dispersion are the ideal precursor for fabrication of free-standing MoS_2 films. In addition, these Li-intercalation exfoliated MoS_2 nanosheets contain a high ratio of metallic 1T phase,[17] which can electrochemically intercalate with various ions, resulting in high capacitive performance. The 1T-MoS_2 film via filtration delivered a volumetric capacitance ranging from 400 to 700 F cm^{-3} in aqueous electrolytes.[17] However, this film was used with the aid of a mechanical support of a gold coated substrate. Probably the free-standing film was lacking in mechanical

robustness and flexibility due to the small lateral size of MoS_2 nanosheets (typically < 1 μm) and the relatively low aspect ratio.[18] The large size of liquid-crystal MoS_2 may provide a solution.[19] Moreover, the restacking of MoS_2 nanosheets may result in a poor capacitive performance especially for thick films, due to the loss of surface area. The introduction of supportive materials such as graphene can enhance the mechanical as well as electrochemical properties. For example, three-dimensional MoS_2/graphene aerogel prepared by a hydrothermal procedure could deliver a specific capacitance of 268 F g^{-1} at 0.5 A g^{-1}. A free-standing and flexible MoS_2/GO hybrid film via vacuum filtration[18] has shown a high volumetric capacitance (~ 380 F cm^{-3} at 10 mV s^{-1}).

Conjugated polymers (CPs) are an intriguing class of materials to form high performance composites with a variety of materials (*e.g.* metal oxides, organic conductors, 2D materials) for supercapacitor applications.[20-22] The composites based on CPs and 2D materials exhibit properties of each of the individual components with synergistic effect due to the facile charge transfer between these two constituents.[23] The addition of CPs to 2D semiconductors (*i.e.* MoS_2 in this work) is valuable because CPs can function as the conducting platform for charge delivery between 2D sheets. The reported composites include MoS_2/polyaniline,[24] MoS_2/polypyrrole[14] and MoS_2/poly(3,4-ethylenedioxythiophene) composites[25], demonstrating high capacitances in the range of 400-700 F g^{-1}. However, these composites are all in the powder form. The reports on free-standing flexible MoS_2-CPs films are still limited. The widely used poly(3,4-ethylenedioxythiophene):poly(styrenesulfonate) (PEDOT:PSS) possesses all the above mentioned advantages for supercapacitor application.[26] More importantly, it can be easily dispersed into different solvents.[27] This unique character allows it to be easily mixed with MoS_2 dispersion forming MoS_2/PEDOT composites and a free-standing flexible film may be produced via simply casting or filtration.

Herein, free-standing MoS_2/PEDOT hybrid films were fabricated through a simple filtration technique. The resultant MoS_2/PEDOT films were robust, demonstrating a high fracture strength of 18.0 MPa. They could deliver high volumetric capacitances and good cycling stability as well. Moreover, this hybrid film had demonstrated its application in all-solid-state bendable devices. This work provides a step forward to the practical application of MoS_2-based electrodes in flexible supercapacitors.

2. Experimental

2.1. Materials

Molybdenum disulfide fine powder was sourced from Asbury Carbon. Poly(3,4-ethylenedioxythiophene):polystyrene sulfonate (PEDOT: PSS) pellets were obtained from Agfa Group. N-butyllithium (2.5 M solution in hexane) was purchased from Sigma-Aldrich.

2.2. Fabrication of MoS_2 nanosheets in aqueous dispersion

Chemically exfoliated MoS_2 nanosheets were prepared using lithium intercalation-exfoliation method developed by Morrison and co-workers.[28] Briefly, dried MoS_2 powder (1g) was put into a 100 mL round-bottom flask, followed by the addition of 2.5 M n-butyllithium solution (10 mL). This mixture was stirred for 48 h under the protection of argon. Then the Li-intercalated MoS_2 was exfoliated into water (~100 mL) via sonication. The resulting dispersion of exfoliated MoS_2 nanosheets was purified by dialysis with water for 2 weeks, removing the contained lithium ions and organic residues.

2.3. Fabrication of MoS_2/PEDOT hybrid films

The MoS_2 nanosheet dispersion (~1 mg mL^{-1}, 60 mL) was added dropwise to 1.5 wt% PEDOT:PSS dispersions (4 mL, 2 mL or 0.8 mL) under stirring to fabricate the films with a weight ratio of 1:1, 2:1 and 5:1 (MoS_2 : PEDOT:PSS). The mixture was then filtered onto a

PVDF hydrophobic filter membrane (90 mm diameter, pore size of 0.22 μm) and peeled off. The complete incorporation of PEDOT:PSS can be evidenced by the clear filtrate produced during the filtration process, as the dispersion containing tiny amount of PEDOT:PSS is light blue in color. These films were dried in a vacuum oven at 60 ^{o}C overnight. They were denoted as MoS_2/PEDOT-1, MoS_2/PEDOT-2 and MoS_2/PEDOT-5 according to the above-mentioned weight ratio. As control samples, neat MoS_2 films were fabricated using the same amount of MoS_2 nanosheets dispersion via the same procedure but on a 47 mm-diameter membrane instead, due to the difficulty in forming robust freestanding films on a 90 mm membrane. Neat PEDOT:PSS films were fabricated by a simple casting technique.

2.4. Structural and morphological characterization

The topographic data of exfoliated MoS_2 nanosheets were collected by atomic force microscopy (AFM) (Asylum Research, MFP-3D). Transmission electron microscopy (TEM) images of MoS_2 nanosheets were collected using JEOL JEM-2200FS. The morphology of the films was characterized with field emission scanning electron microscopy (FE-SEM) (JEOL JSM-7500FA). Raman spectra were obtained with a confocal Raman spectrometer (Jobin Yvon HR800, Horiba) using a 632.8 nm diode laser. X-ray photoelectron spectroscopy (XPS) data was collected from a hemispherical energy PHOIBOS 100/150 analyser. Tensile tests of the films were conducted using a Shimadzu EZ mechanical tester at a cross-head speed of 1 mm/min.

2.5. Supercapacitors assembly and electrochemical measurements

Symmetrical supercapacitors were assembled into two-electrode Swagelok type cells with filter paper as separator and 1 M Na_2SO_4 as electrolyte. The films were cut into a dimension of 0.5 cm × 0.5 cm for use.

For an all-solid-state supercapacitor, a PVA/H_3PO_4 gel electrolyte (PVA:H_3PO_4, 1:1.5) was used following the previously reported procedure.[29] A film electrode (1 cm × 2 cm) was pasted onto a stainless steel mesh with silver paste (Electron Microscope Sciences Co.), followed by being immersed in the electrolyte overnight. Two electrodes with the semi-dried electrolyte layer were pressed together forming flexible devices.

Cyclic voltammetry (CV) of the device was conducted from 0 to 1 V using a CHI 604D (CHI Instruments). Electrochemical impedance spectra were obtained using a Gamry EIS 3000 system over the frequency range of 100 kHz to 0.01 Hz with an AC perturbation of 10 mV at open circuit potential. Galvanostatic charge/discharge tests of the devices were performed using a battery test system (Neware Electronic Co.) between 0 and 1 V.

3. Results and discussion

The exfoliated MoS_2 nanosheets show a lateral sheet size of 100-200 nm (Fig. 1a). The height profile displays a thickness of around 1.0 nm (Fig. 1b). The nanosheet with a ~2.0 nm thickness can also be observed, indicating a 2-3 layered structure. The thickness of a mechanically exfoliated MoS_2 monolayer is typically 0.65~0.70 nm.[30, 31] The variation in thickness can be ascribed to the surface corrugation due to distortions, the presence of adsorbed or trapped molecules.[32] The TEM image further reveals a layered structure of the exfoliated MoS_2 nanosheets (Figure 1c). A typical few-layer MoS_2 nanosheet can be observed with an average interlayer distance of 0.66 nm.

The pristine PEDOT:PSS film shows a compact and featureless cross-sectional view (Fig. 2a). Within a free-standing MoS_2 film, MoS_2 nanosheets restacked on top of each other forming a typical layered structure (Fig. 2b). With the introduction of PEDOT:PSS into the system, it still retains a layered structure (Fig. 2c-e). At higher magnification, no distinct gaps can be found between the nanosheets assembly within the hybrid film (MoS_2/PEDOT-2) as that for

MoS_2 (Fig. 2f, 2g). This may be explained by that the polymer PEDOT acts as glue connecting MoS_2 sheets together. All the elements Mo, S and C were uniformly distributed within the MoS_2/PEDOT-2 film, as evidenced from the energy dispersive X-ray spectroscopy (EDS) results (Figure S1), indicating the even distribution of PEDOT:PSS in the hybrid film. In comparison, no C element can be detected on the cross-section of the neat MoS_2 film. Neat MoS_2, neat PEDOT:PSS, MoS_2/PEDOT-1, MoS_2/PEDOT-2 and MoS_2/PEDOT-5, demonstrated a respective thicknesses of 9.5 μm, 9.6 μm, 9.3 μm, 7.0 μm and 4.5 μm. The corresponding density (ρ) was 3.56 g cm^{-3}, 1.60 g cm^{-3}, 1.79 g cm^{-3}, 1.96 g cm^{-3} and 2.22 g cm^{-3}.

The reinforcement effect of PEDOT:PSS on the mechanical properties of the hybrid films was characterized by tensile tests (Fig. 2f). The neat MoS_2 film displayed very poor mechanical properties with a fracture strength of only 5.3 MPa and a maximum elongation of 0.3%, due to the relatively small lateral size of MoS_2 sheets and lack of strong interactions between the restacked layers. With the incorporation of PEDOT:PSS (~20%), MoS_2/PEDOT-5 film displayed an improved mechanical strength of 7.4 MPa (39.5% increase). The mechanical properties of these hybrid films were dramatically improved with the increased amount of PEDOT:PSS. The MoS_2/PEDOT-1 (~50% PEDOT) and MoS_2/PEDOT-2 (~33% PEDOT) films exhibited a fracture strength of 23.5 MPa and 18.0 MPa, a 341% and 238% increase, respectively. The respective maximum elongation was also increased to 1.4% and 0.9%, a 442% and 262% increase. These films are robust, as demonstrated in Fig. 2f (inset). The detailed mechanical properties are summarized in Table 1 for clarity. The mechanical strength of these two hybrid films (MoS_2/PEDOT-1 and MoS_2/PEDOT-2) is higher than or comparable to that of the previously reported flexible MoS_2 or graphene based films, including MoS_2/GO hybrid film (65 MPa),[18] graphene-cellulose paper (8.67 MPa)[33] and graphene/polypyrrole nanofiber films (35.0 MPa)[34]. Not surprisingly, neat PEDOT:PSS

film possessed the best tensile performance with the highest fracture strength of 35.9 MPa and maximum elongation of 3.8%. The incorporation of PEDOT:PSS, cannot only benefit the mechanical properties, but also enhance the electrical conductivity (Table 1). These hybrid films exhibited at least one order of magnitude higher conductivities (17.9, 11.9 and 4.4 S cm^{-1} for MoS_2/PEDOT-1, 2 and 5 film) than that of the neat MoS_2 film (0.5 S cm^{-1}). Such improvement may be attributed to enhanced electron transport along the conducting polymer chains that form a conductive matrix within the hybrid film.

The chemical structure of bulk MoS_2, chemically-exfoliated MoS_2 and hybrid films was studied by Raman spectroscopy. Bulk MoS_2 showed two characteristic peaks at 382.2 cm^{-1} and 406.6 cm^{-1} (Fig. 3a), which can be assigned to the in-plane (E^1_{2g}) and out-of-plane (A_{1g}) vibration modes, respectively.[35, 36] Upon chemical exfoliation, a blueshift of E^1_{2g} and A_{1g} peak to 375.5 cm^{-1} and 402.0 cm^{-1} was observed for the restacked MoS_2 film, indicating that the exfoliated MoS_2 had undergone partial phase transition from 2H to 1T.[37, 38] These blueshifts can also be found in hybrid films, suggesting that the 1T component of the exfoliated MoS_2 was well maintained after being hybridized with PEDOT:PSS.[32]

X-ray photon spectroscopy (XPS) results further supported this phase transition of MoS_2 before and after exfoliation. In the case of bulk MoS_2, there exists two narrow peaks at 232.8 eV and 229.6 eV in the Mo 3d binding region (Fig. 3b), corresponding to Mo $3d_{3/2}$ and Mo $3d_{5/2}$ respectively, indicating the +4 oxidation state of 2H-phase MoS_2.[19, 39, 40] Upon chemical exfoliation, these two peaks are broadened. The deconvolution of these peaks shows two more peaks located at 231.8 eV and 228.5 eV, which suggests that the structure of MoS_2 has partially transformed from 2H phase to 1T phase.[32] The ratio between 1T phase and 2H phase in the exfoliated MoS_2 can be quantified by fitting the deconvoluted peak areas. The 1T: 2H ratio in neat MoS_2 film is ~1:1, which means that about half of the 2H-phase MoS_2 have been converted into 1T phase. For the hybrid films similar deconvoluted peaks assigned to

1T-phase MoS_2 can be observed. The 1T:2H ratio in MoS_2/PEDOT-2 film is ~0.96:1, very close to that of neat MoS_2 film, indicating the well-retained structure of exfoliated MoS_2. The oxidation of MoS_2 in these hybrid films can also be noticed, as evidenced by a new small peak at 235.2 eV corresponding to Mo^{6+} $3d_{5/2}$.[41]

The CV curves of MoS_2/PEDOT-2 hybrid film and neat film electrodes at a scan rate of 50 mV s^{-1} are illustrated in Fig. 4a. The capacitive performance was investigated in a two-electrode configuration, which is a closer arrangement to a practical device. The MoS_2/PEDOT-2 film exhibited significantly higher current response than neat MoS_2 and PEDOT:PSS, indicating a much higher capacitance to deliver. The densely restacked structure of MoS_2 film could hinder the diffusion of electrolyte ions into the interior of the film, leading to a poor utilization of the material and low capacitance, as demonstrated for graphene-based materials.[42, 43] The presence of highly conductive PEDOT:PSS could not only prevent MoS_2 nanosheets from restacking, but also facilitate the charge delivery between the MoS_2 nanosheets. MoS_2/PEDOT-2 film displayed nearly rectangular CV shapes even at a high scan rate of 100 mV s^{-1} (Fig. 4b), demonstrating an excellent capacitive behaviour. For neat MoS_2, the distortion of the curves can be clearly seen when the scan rate reaches 50 mV s^{-1} (Fig. 4c), which may be ascribed to its low conductivity.

The supercapacitors based on MoS_2/PEDOT-2 films showed nearly linear and symmetric charge/discharge curves at the applied current densities range of 0.2 to 4 A g^{-1} (Fig. 4d), indicating an excellent reversibility. These hybrid films delivered much larger volumetric capacitances than neat MoS_2 or PEDOT:PSS film at a current density of 0.2 A g^{-1} (Fig. 4e). The current applied was based on the total mass of both film electrodes. The volumetric capacitance of a single electrode was calculated using the equation of $C_V=\rho\times C_g=\rho\times(4\times i\times t)/(m\times \Delta V)$, where C_V is the volumetric capacitance in F cm^{-3}, ρ is the density of the films in g cm^{-3}, C_g is the gravimetric capacitance in F g^{-1}, i is the discharge

current in A, *t* is the discharge time in s, *m* is the total mass of the two electrodes in g and ΔV is the scan potential window in V. These hybrid films present enhanced volumetric capacitances (C_V) (Fig. 4f). The largest C_V (141.4 F cm^{-3}) was delivered by MoS_2/PEDOT-2 film at a current density of 0.2 A g^{-1}, much higher than that of neat MoS_2 (59.9 F cm^{-3}) and neat PEDOT:PSS (44.8 F cm^{-3}) films at the same current density. At a high current density of 4 A g^{-1}, MoS_2/PEDOT-2 film could still afford a capacitance of 94.3 F cm^{-3}, showing a capacitance retention ratio of 66.7%, whilst neat MoS_2 and PEDOT:PSS films display a lower retention ratio of 54.1% and 54.0%, respectively. This enhanced capacitive performance can be attributed to the incorporation of PEDOT:PSS between MoS_2 nanosheets, hence improving the conductivity and charge transfer.

The cycling performance of the film electrodes was investigated at a current density of 1 A g^{-1}. Both neat PEDOT:PSS and neat MoS_2 films showed a capacitance drop of over 10% in the first 2000 cycles (Fig. 4g). At the 5000th cycle, the former offered a capacitance retention rate of 85.0%, while the latter only retained 73.4% of its initial capacitance. In contrast, MoS_2/PEDOT-2 electrode only showed a slight volumetric capacitance loss over 5000 cycles. The retained capacitance was 116.2 F cm^{-3}, 98.6% of the initial capacitance (117.8 mF cm^{-3}), suggesting its excellent cycling stability. Such cycling performance is superior to the reported MoS_2-conjugated polymer composite electrodes, such as 90% retention after 1000 cycles for MoS_2/PEDOT composites[25] or 85% after 4000 cycles for MoS_2/polypyrrole composites[14]. It is also higher than the reported MoS_2/GO films (95% after 10000 cycles at 300 mV s^{-1}).[18] These cells were disassembled for investigation. Compared to the pristine films, cracks were generated on the MoS_2 film after electrochemical cycling (Figure S2a, b), while the MoS_2/PEDOT-2 film still remained intact (Figure S2c, d). This clearly suggests improved mechanical integrity in the hybrid film, leading to good cycling stability.

The volumetric energy density and power density of the devices were calculated using the equations of $E=[C_V\times(\Delta V)^2]/(2\times4\times3600)$ and $P=(3600\times E)/t$, where E is the volumetric energy density in Wh cm^{-3}, P is the volumetric power density in W cm^{-3}. The device based on MoS_2/PEDOT-2 films presented a volumetric energy density of 4.9 mWh cm^{-3} at a volumetric power density of 0.19 W cm^{-3}. At the highest discharge current density, MoS_2/PEDOT-2 could still deliver a volumetric power density of 3.9 W cm^{-3} with an energy density of 3.3

Wh cm^{-3}. The Ragone plot of the supercapacitors based on MoS_2/PEDOT-2 electrodes and the results from some recently reported MoS_2-based supercapacitors are shown in Fig. 4h. The 1T-MoS_2 film displayed a superior energy density of up to 16 mWh cm^{-3} in aqueous electrolyte.[17] This may be ascribed to its high content of 1T-MoS_2 nanosheets (~70%) and the low thickness of the film, only ~1 μm. It should be pointed out that the film thickness can dramatically influence the capacitive performance, since a higher ion diffusion length in the thick film leads to lower charge/discharge rates and power densities.[44] The thicknesses of our films are close to those of commercial cell electrodes, which are in the range of 10 to several hundreds of microns.[45, 46] The energy densities obtained using MoS_2/PEDOT films are also higher than or comparable to that of MoS_2/GO composites[18] and directly deposited MoS_2 thin film[47], thermally reduced graphene oxide-based microsupercapacitors (TG MSCs)[48] or methane-plasma-treated graphene-based microsupercapacitors (MPG MSCs)[48]. These results are also higher than observed with conventional electrolytic capacitors[49] and lithium thin film batteries,[50] suggesting its potential applications as a practical supercapacitor electrode. We should also point out that our free-standing MoS_2/PEDOT films possess better electrochemical performance and remarkably enhanced mechanical robustness and flexibility compared to those reported for MoS_2/graphene films[18]

and graphene/polymer films[33, 34] suggesting that use in flexible energy storage devices is viable.

Nyquist plots of electrochemical impedance spectroscopy (EIS) for these film electrodes are depicted in Fig. 5a. The simulated equivalent circuit consists of four elements (inset of Fig. 5a): bulk resistance (R_s), charge-transfer resistance (R_{ct}), Warburg impedance (W) and constant phase element (CPE). The detailed values of each element are listed in **Table S1** (see supporting information). The hybrid films have a much smaller R_{ct} (50.6, 57.8 and 69.5 Ω for MoS_2/PEDOT-1, 2 and 5 respectively) than that of neat films (106.7 Ω). The linear parts at the low frequency region are related to the ion diffusion process. It can be seen that all the hybrid films displayed nearly vertical lines (>80^o with *Z'* axis), indicating a nearly ideal capacitive behaviour.[51] In contrast, neat MoS_2 film displayed a ~45^o linear part, indicating the high diffusion resistance of ions in the structure of the electrodes.[52] These results clearly demonstrate that these hybrid films can allow faster ion diffusion and charge transport, which leads to the greatly improved electrochemical properties (*e.g.* rate performance) as demonstrated.

To investigate the potential application of these hybrid films in flexible devices, the MoS_2/PEDOT-2 films were further assembled into all-solid-state supercapacitors. The device (inset of Fig. 5b) was tested at a scan rate of 50 mV s^{-1} from 0 to 1 V under different bending angles (Fig. 5b). The volumetric capacitances of the single electrode were calculated using the equation: $C_V = \rho \times C_g = \frac{\rho}{mv\Delta V}\int IdV$, where, v is the scan rate in V s^{-1}, ΔV is the potential window in V and I is the current in A. At the relaxation (unbent) state, the MoS_2/PEDOT-2 films supercapacitor delivered a C_V of 156.3 F cm^{-3}. When being bent to 90^o, it displayed a well remained CV curve offering a capacitance of 150.9 F cm^{-3}, and a high capacitance retention rate of 96.6%. Even upon a 180^o bending, the hybrid film still delivered a C_V of

137.2 F cm^{-3}, a retention rate of 87.8%. This device was subjected to a bending process for up to 1000 times at 90^{o}, no significant changes can be observed (Fig. 5c). It could still deliver a volumetric capacitance of 125.1 F cm^{-3}, 80.0% of that obtained from the initial unbent state. The robustness and durability are very important features for practical bendable/flexible supercapacitors. This proven integrity of these hybrid films against repeated bending indicates that they are promising electrodes for use as flexible supercapacitors.

4. Conclusions

Free-standing MoS_2/PEDOT hybrid films were developed by simply incorporating PEDOT:PSS into the chemically exfoliated MoS_2 nanosheets via a simple vacuum filtration technique. These hybrid films showed substantially enhanced mechanical properties compared to neat MoS_2 film, which can be explained by that the polymer PEDOT acted as glue between the MoS_2 nanosheets. The robustness and flexibility of these electrodes could also be evidenced by the electrode integrity being retained over 1000 bending cycles. The highly conductive and hydrophilic PEDOT:PSS also effectively improved the conductivity and charge delivery, resulting in greatly improved electrochemical properties. The MoS_2/PEDOT-2 hybrid film exhibited a large volumetric capacitance of 141.4 F cm^{-3}, a capacitance retention ratio of 98.6% over 5000 cycles and a volumetric energy density of 4.9 mWh cm^{-3}. The combination of good capacitive performance and mechanical properties suggests its promising use for high-performance flexible supercapacitors.

Acknowledgements

Funding from the Australian Research Council Centre of Excellence Scheme (Project Number CE 140100012) is gratefully acknowledged. G.G.W. is grateful to the ARC for

support under the Australian Laureate Fellowship scheme (FL110100196). The authors would like to thank the Australian National Fabrication Facility-Materials node (ANFF) and the UOW Electron Microscopy Centre for the equipment use.

References

[1] H. Nishide, K. Oyaizu, Toward flexible batteries, Science 319 (2008) 737-738.

[2] X. Lu, Y. Xia, Electronic materials: Buckling down for flexible electronics, Nat. Nano. 1 (2006) 163-164.

[3] C. Wang, G.G. Wallace, Flexible electrodes and electrolytes for energy storage, Electrochim. Acta. 175 (2015) 87-95.

[4] R. Kötz, M. Carlen, Principles and applications of electrochemical capacitors, Electrochim. Acta 45 (2000) 2483-2498.

[5] J.R. Miller, P. Simon, Electrochemical capacitors for energy management, Science 321 (2008) 651-652.

[6] H. Chen, M.B. Muller, K.J. Gilmore, G.G. Wallace, D. Li, Mechanically strong, electrically conductive, and biocompatible graphene paper, Adv. Mater. 20 (2008) 3557-3561.

[7] C.Y. Wang, D. Li, C.O. Too, G.G. Wallace, Electrochemical properties of graphene paper electrodes used in lithium batteries, Chem. Mater. 21 (2009) 2604-2606.

[8] Y. Ge, C. Wang, K. Shu, C. Zhao, X. Jia, S. Gambhir, G.G. Wallace, A facile approach for fabrication of mechanically strong graphene/polypyrrole films with large areal capacitance for supercapacitor applications, Rsc Adv. 5 (2015) 102643-102651.

[9] I. Sultana, M.M. Rahman, J. Wang, C. Wang, G.G. Wallace, H.-K. Liu, All-polymer battery system based on polypyrrole (PPy)/para (toluene sulfonic acid) (pTS) and polypyrrole (PPy)/indigo carmine (IC) free standing films, Electrochim. Acta 83 (2012) 209-215.

[10] F. Schedin, A.K. Geim, S.V. Morozov, E.W. Hill, P. Blake, M.I. Katsnelson, K.S. Novoselov, Detection of individual gas molecules adsorbed on graphene, Nat. Mater. 6 (2007) 652-655.

[11] C.-C. Hu, K.-H. Chang, M.-C. Lin, Y.-T. Wu, Design and tailoring of the nanotubular arrayed architecture of hydrous RuO_2 for next generation supercapacitors, Nano Lett. 6 (2006) 2690-2695.

[12] K.-J. Huang, J.-Z. Zhang, G.-W. Shi, Y.-M. Liu, Hydrothermal synthesis of molybdenum disulfide nanosheets as supercapacitors electrode material, Electrochim. Acta 132 (2014) 397-403.

[13] J. Kibsgaard, Z. Chen, B.N. Reinecke, T.F. Jaramillo, Engineering the surface structure of MoS_2 to preferentially expose active edge sites for electrocatalysis, Nat. Mater. 11 (2012) 963-969.

[14] H. Tang, J. Wang, H. Yin, H. Zhao, D. Wang, Z. Tang, Growth of polypyrrole ultrathin films on MoS_2 monolayers as high-performance supercapacitor electrodes, Adv. Mater. 27 (2015) 1117-1123.

[15] K.-J. Huang, L. Wang, J.-Z. Zhang, L.-L. Wang, Y.-P. Mo, One-step preparation of layered molybdenum disulfide/multi-walled carbon nanotube composites for enhanced performance supercapacitor, Energy 67 (2014) 234-240.

[16] J.M. Soon, K.P. Loh, Electrochemical double-layer capacitance of MoS_2 nanowall films, Electrochem. and Solid-State Lett. 10 (2007) A250-A254.

[17] M. Acerce, D. Voiry, M. Chhowalla, Metallic 1T phase MoS_2 nanosheets as supercapacitor electrode materials, Nat. Nano. 10 (2015) 313-318.

[18] S. Byun, D.M. Sim, J. Yu, J.J. Yoo, High-power supercapacitive properties of graphene oxide hybrid films with highly conductive molybdenum disulfide nanosheets, Chemelectrochem 2 (2015) 1938-1946.

[19] R. Jalili, S. Aminorroaya-Yamini, T.M. Benedetti, S.H. Aboutalebi, Y. Chao, G.G. Wallace, D.L. Officer, Processable 2D materials beyond graphene: MoS_2 liquid crystals and fibres, Nanoscale 8 (2016) 16862-16867.

[20] R. Jalili, J.M. Razal, P.C. Innis, G.G. Wallace, One-step wet-spinning process of poly(3,4-ethylenedioxythiophene):poly(styrenesulfonate) fibers and the origin of higher electrical conductivity, Adv. Funct. Mater. 21 (2011) 3363-3370.

[21] R. Jalili, J.M. Razal, G.G. Wallace, Exploiting high quality PEDOT:PSS-SWNT composite formulations for wet-spinning multifunctional fibers, J. Mater. Chem. 22 (2012) 25174-25182.

[22] R. Jalili, J.M. Razal, G.G. Wallace, Wet-spinning of PEDOT:PSS/functionalized-SWNTs composite: a facile route toward production of strong and highly conducting multifunctional fibers, Sci Rep-Uk 3 (2013) 3438.

[23] K.S.U. Schirmer, D. Esrafilzadeh, B.C. Thompson, A.F. Quigley, R.M.I. Kapsa, G.G. Wallace, Conductive composite fibres from reduced graphene oxide and polypyrrole nanoparticles, Journal of Materials Chemistry B 4 (2016) 1142-1149.

[24] K.-J. Huang, L. Wang, Y.-J. Liu, H.-B. Wang, Y.-M. Liu, L.-L. Wang, Synthesis of polyaniline/2-dimensional graphene analog MoS_2 composites for high-performance supercapacitor, Electrochim. Acta 109 (2013) 587-594.

[25] J. Wang, Z. Wu, H. Yin, W. Li, Y. Jiang, Poly(3,4-ethylenedioxythiophene)/MoS_2 nanocomposites with enhanced electrochemical capacitance performance, Rsc Adv. 4 (2014) 56926-56932.

[26] Y. Liu, B. Weng, J.M. Razal, Q. Xu, C. Zhao, Y. Hou, S. Seyedin, R. Jalili, G.G. Wallace, J. Chen, High-performance flexible all-solid-state supercapacitor from large free-standing graphene-PEDOT/PSS films, Sci Rep-Uk 5 (2015) 17045.

[27] X. Crispin, F.L.E. Jakobsson, A. Crispin, P.C.M. Grim, P. Andersson, A. Volodin, C. van Haesendonck, M. Van der Auweraer, W.R. Salaneck, M. Berggren, The origin of the high conductivity of poly(3,4-ethylenedioxythiophene)−poly(styrenesulfonate) (PEDOT−PSS) plastic electrodes, Chem. Mater. 18 (2006) 4354-4360.

[28] P. Joensen, R.F. Frindt, S.R. Morrison, Single-layer MoS_2, Mater. Res. Bull. 21 (1986) 457-461.

[29] C. Zhao, C. Wang, Z. Yue, K. Shu, G.G. Wallace, Intrinsically stretchable supercapacitors composed of polypyrrole electrodes and highly stretchable gel electrolyte, Acs Appl. Mater. Inter. 5 (2013) 9008-9014.

[30] S. Ghatak, A.N. Pal, A. Ghosh, Nature of electronic states in atomically thin MoS_2 field-effect transistors, Acs Nano 5 (2011) 7707-7712.

[31] RadisavljevicB, RadenovicA, BrivioJ, GiacomettiV, KisA, Single-layer MoS_2 transistors, Nat. Nano. 6 (2011) 147-150.

[32] G. Eda, H. Yamaguchi, D. Voiry, T. Fujita, M. Chen, M. Chhowalla, Photoluminescence from chemically exfoliated MoS_2, Nano Lett. 11 (2011) 5111-5116.

[33] Z. Weng, Y. Su, D.-W. Wang, F. Li, J. Du, H.-M. Cheng, Graphene–cellulose paper flexible supercapacitors, Adv. Energy Mater. 1 (2011) 917-922.

[34] S. Li, C. Zhao, K. Shu, C. Wang, Z. Guo, G.G. Wallace, H. Liu, Mechanically strong high performance layered polypyrrole nano fibre/graphene film for flexible solid state supercapacitor, Carbon 79 (2014) 554-562.

[35] C. Lee, H. Yan, L.E. Brus, T.F. Heinz, J. Hone, S. Ryu, Anomalous lattice vibrations of single- and few-layer MoS_2, Acs Nano 4 (2010) 2695-2700.

[36] H. Li, Q. Zhang, C.C.R. Yap, B.K. Tay, T.H.T. Edwin, A. Olivier, D. Baillargeat, From bulk to monolayer MoS_2: Evolution of raman scattering, Adv. Funct. Mater. 22 (2012) 1385-1390.

[37] H. Zeng, J. Dai, W. Yao, D. Xiao, X. Cui, Valley polarization in MoS_2 monolayers by optical pumping, Nat. Nano. 7 (2012) 490-493.

[38] H. Wang, Z. Lu, S. Xu, D. Kong, J.J. Cha, G. Zheng, P.-C. Hsu, K. Yan, D. Bradshaw, F.B. Prinz, Y. Cui, Electrochemical tuning of vertically aligned MoS_2 nanofilms and its application in improving hydrogen evolution reaction, Proceedings of the National Academy of Sciences 110 (2013) 19701-19706.

[39] D. Voiry, M. Salehi, R. Silva, T. Fujita, M. Chen, T. Asefa, V.B. Shenoy, G. Eda, M. Chhowalla, Conducting MoS_2 nanosheets as catalysts for hydrogen evolution reaction, Nano Lett. 13 (2013) 6222-6227.

[40] X. Shao, J. Tian, Q. Xue, C. Ma, Fabrication of MoO_3 nanoparticles on an MoS_2 template with $(C_4H_9Li)MoS_2$ exfoliation, J. Mater. Chem. 13 (2003) 631-633.

[41] Z. Zeng, T. Sun, J. Zhu, X. Huang, Z. Yin, G. Lu, Z. Fan, Q. Yan, H.H. Hng, H. Zhang, An effective method for the fabrication of few-layer-thick inorganic nanosheets, Angewandte Chemie International Edition 51 (2012) 9052-9056.

[42] B.G. Choi, J. Hong, W.H. Hong, P.T. Hammond, H. Park, Facilitated ion transport in all-solid-state flexible supercapacitors, Acs Nano 5 (2011) 7205-7213.

[43] Q. Wu, Y. Xu, Z. Yao, A. Liu, G. Shi, Supercapacitors based on flexible graphene/polyaniline nanofiber composite films, Acs Nano 4 (2010) 1963-1970.

[44] G. Xiong, C. Meng, R.G. Reifenberger, P.P. Irazoqui, T.S. Fisher, A review of graphene-based electrochemical microsupercapacitors, Electroanal. 26 (2014) 30-51.

[45] M.D. Stoller, R.S. Ruoff, Best practice methods for determining an electrode material's performance for ultracapacitors, Energ. Environ. Sci. 3 (2010) 1294-1301.

[46] S. Zhang, N. Pan, Supercapacitors performance evaluation, Adv. Energy Mater. 5 (2015) 1401401.

[47] N. Choudhary, M. Patel, Y.-H. Ho, N.B. Dahotre, W. Lee, J.Y. Hwang, W. Choi, Directly deposited MoS_2 thin film electrodes for high performance supercapacitors, J. Mater. Chem. A 3 (2015) 24049-24054.

[48] Z.S. Wu, K. Parvez, X. Feng, K. Müllen, Graphene-based in-plane micro-supercapacitors with high power and energy densities, Nat. Commun. 4 (2013).

[49] M.F. El-Kady, V. Strong, S. Dubin, R.B. Kaner, Laser scribing of high-performance and flexible graphene-based electrochemical capacitors, Science 335 (2012) 1326-1330.

[50] D. Pech, M. Brunet, H. Durou, P. Huang, V. Mochalin, Y. Gogotsi, P.-L. Taberna, P. Simon, Ultrahigh-power micrometre-sized supercapacitors based on onion-like carbon, Nat. Nano. 5 (2010) 651-654.

[51] W. Sugimoto, H. Iwata, K. Yokoshima, Y. Murakami, Y. Takasu, Proton and electron conductivity in hydrous ruthenium oxides evaluated by electrochemical impedance spectroscopy: the origin of large capacitance, The Journal of Physical Chemistry B 109 (2005) 7330-7338.

[52] J. Yan, T. Wei, B. Shao, F. Ma, Z. Fan, M. Zhang, C. Zheng, Y. Shang, W. Qian, F. Wei, Electrochemical properties of graphene nanosheet/carbon black composites as electrodes for supercapacitors, Carbon 48 (2010) 1731-1737.

Figure captions

Fig. 1 AFM image (a) and height profile (b) along the line drawn in (a) of exfoliated MoS_2 nanosheets; (c) TEM image of MoS_2 nanosheets.

Fig. 2 Cross-sectional view (a-g) and strain-stress curves (h) of the films. (a) Neat PEDOT:PSS, (b) neat MoS_2, (c) MoS_2/PEDOT-1, (d) MoS_2/PEDOT-2 and (e) MoS_2/PEDOT-5 films. (f, g) Cross-section of MoS_2 and MoS_2/PEDOT-2 films at higher magnification. Inset of (f): a photo of a flexible MoS_2/PEDOT-2 film.

Fig. 3 (a) Raman spectra of bulk MoS_2 powder, MoS_2 film and MoS_2/PEDOT films. (b) XPS spectra of bulk MoS_2 powder, neat MoS_2 and MoS_2/PEDOT-2 film, showing the Mo 3d binding region.

Fig. 4 (a-c) Cyclic voltammograms of the supercapacitor composed of MoS_2/PEDOT-2 (a), and neat MoS_2 films (b) at different scan rates; comparison between these two supercapacitors and that with neat PEDOT:PSS films at a scan rate of 50 mV s^{-1} (c) in 1 M Na_2SO_4. (d) Galvanostatic charge/discharge curves of MoS_2/PEDOT-2 film supercapacitor at different current densities. (e, f) Charge/discharge curves at a current density of 0.2 A g^{-1} (e) and volumetric capacitances as a function of current densities (f) of the supercapacitors composed of these film electrodes. (g) Cycling stability of the supercapacitors based on neat MoS_2, neat PEDOT:PSS and MoS_2/PEDOT-2 film electrodes. (h) Ragone plot of volumetric power and energy densities reported from previously reported MoS_2-based energy storage materials and some commonly applied energy storage devices for comparison with MoS_2/PEDOT-2 film.

Fig. 5 (a) Nyquist plots (symbol) and the simulated curves (line) of neat and hybrid films based supercapacitors in 1 M Na_2SO_4 (inset: the equivalent circuit diagram used to simulate the Nyquist plots). (b) Cyclic voltammograms of MoS_2/PEDOT-2 film based supercapacitor

at different bending angles at a scan rate of 50 mV s^{-1} (inset: photo of the flexible supercapacitor device). (c) Cyclic voltammograms of MoS_2/PEDOT-2 recorded during the bending process.

Fig. 1.

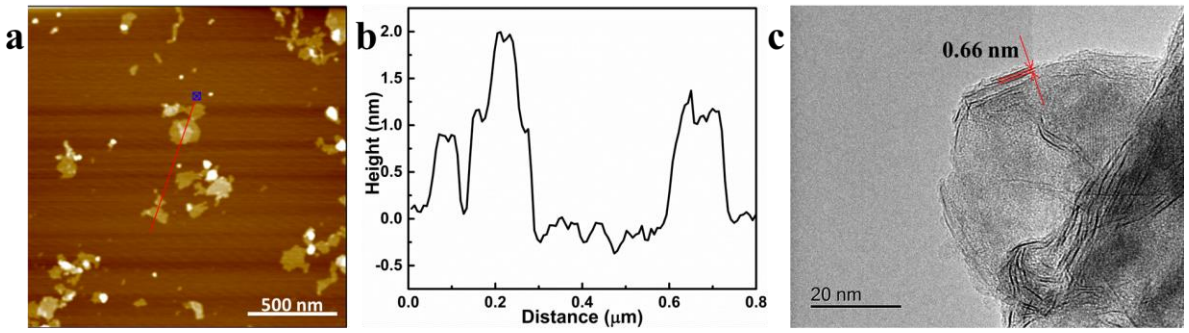

Fig. 2.

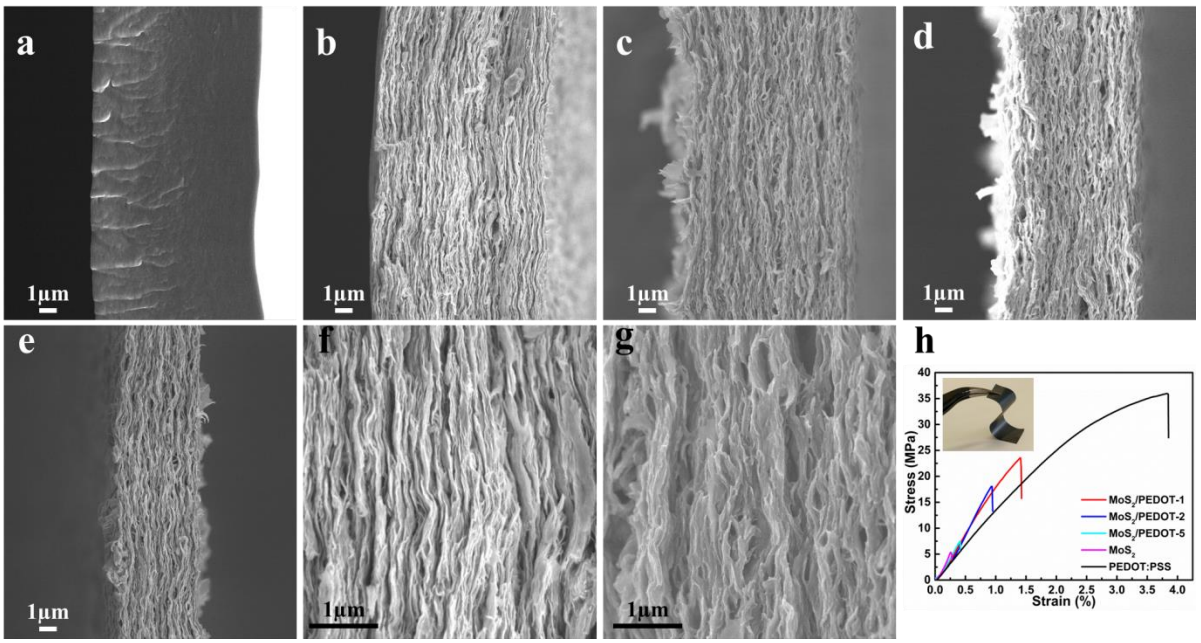

Fig. 3.

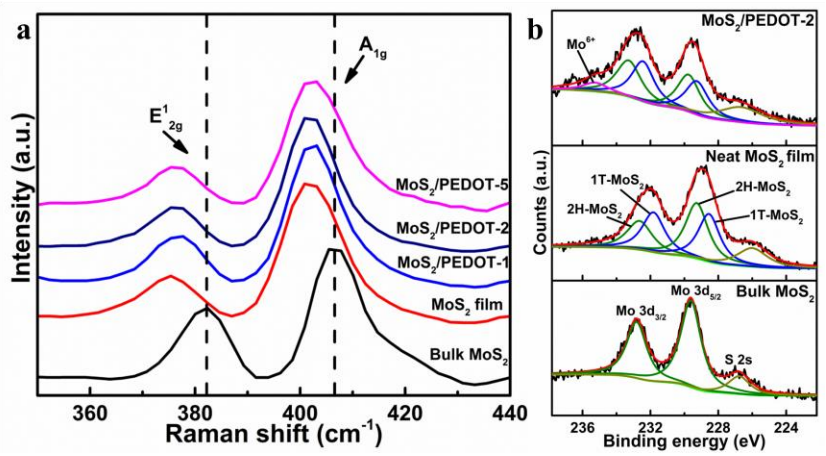
a
b
Intensity (a.u.)
Raman shift (cm-1)
E12g
A1g
MoS2/PEDOT-5
MoS2/PEDOT-2
MoS2/PEDOT-1
MoS2 film
Bulk MoS2
360
380
400
420
440
MoS2/PEDOT-2
Mo6+
Neat MoS2 film
1T-MoS2
2H-MoS2
2H-MoS2
1T-MoS2
Counts (a.u.)
Mo 3d5/2
Bulk MoS2
Mo 3d3/2
S 2s
236
232
228
224
Binding energy (eV)

Fig. 4.

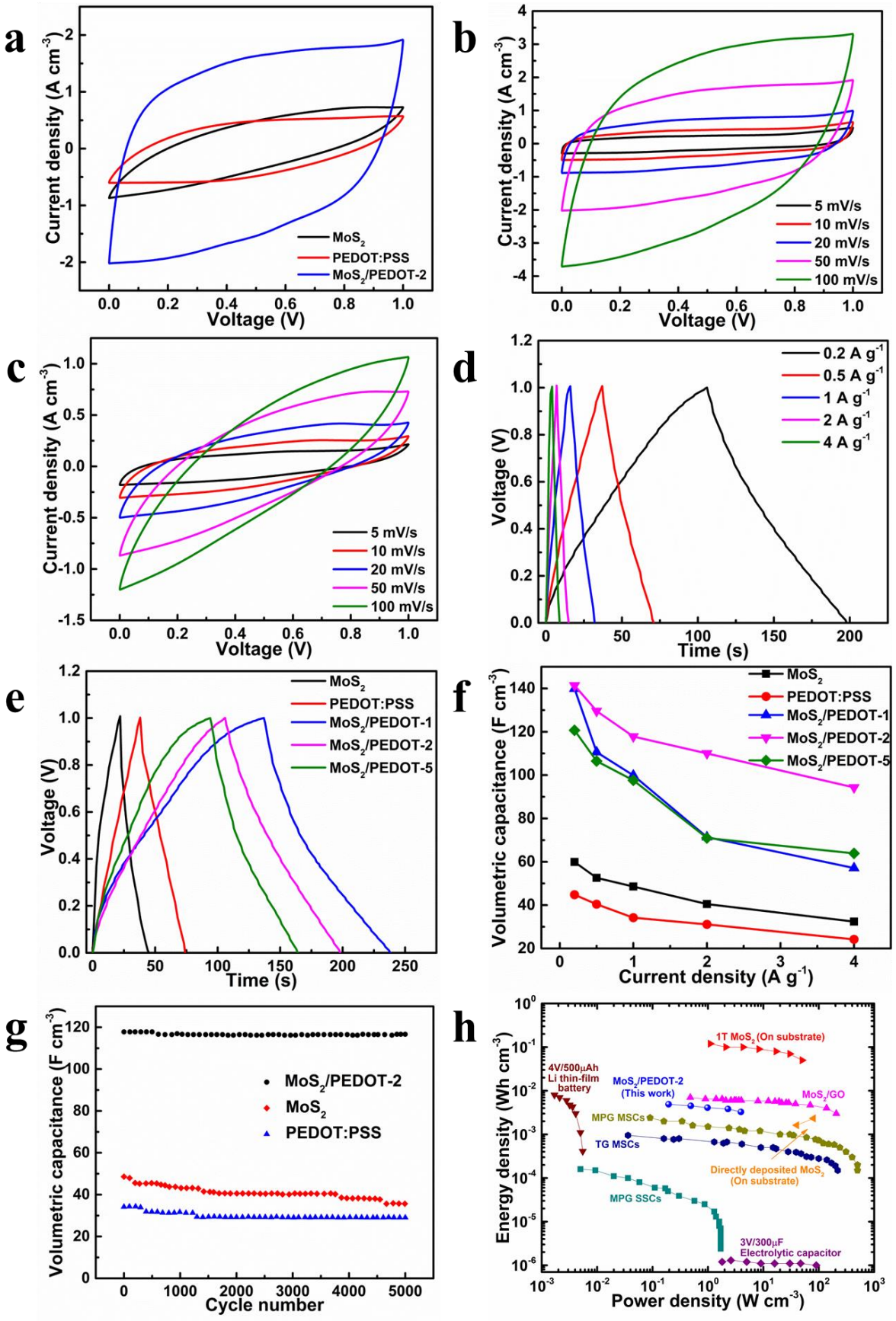
a
Current density (A cm-3)
Voltage (V)
MoS2
PEDOT:PSS
MoS2/PEDOT-2
b
Current density (A cm-3)
Voltage (V)
5 mV/s
10 mV/s
20 mV/s
50 mV/s
100 mV/s
c
Current density (A cm-3)
Voltage (V)
5 mV/s
10 mV/s
20 mV/s
50 mV/s
100 mV/s
d
Voltage (V)
Time (s)
0.2 A g-1
0.5 A g-1
1 A g-1
2 A g-1
4 A g-1
e
Voltage (V)
Time (s)
MoS2
PEDOT:PSS
MoS2/PEDOT-1
MoS2/PEDOT-2
MoS2/PEDOT-5
f
Volumetric capacitance (F cm-3)
Current density (A g-1)
MoS2
PEDOT:PSS
MoS2/PEDOT-1
MoS2/PEDOT-2
MoS2/PEDOT-5
g
Volumetric capacitance (F cm-3)
Cycle number
MoS2/PEDOT-2
MoS2
PEDOT:PSS
h
Energy density (Wh cm-3)
Power density (W cm-3)
1T MoS2 (On substrate)
4V/500μAh Li thin-film battery
MoS2/PEDOT-2 (This work)
MoS2/GO
MPG MSCs
TG MSCs
Directly deposited MoS2 (On substrate)
MPG SSCs
3V/300μF Electrolytic capacitor

Fig. 5.

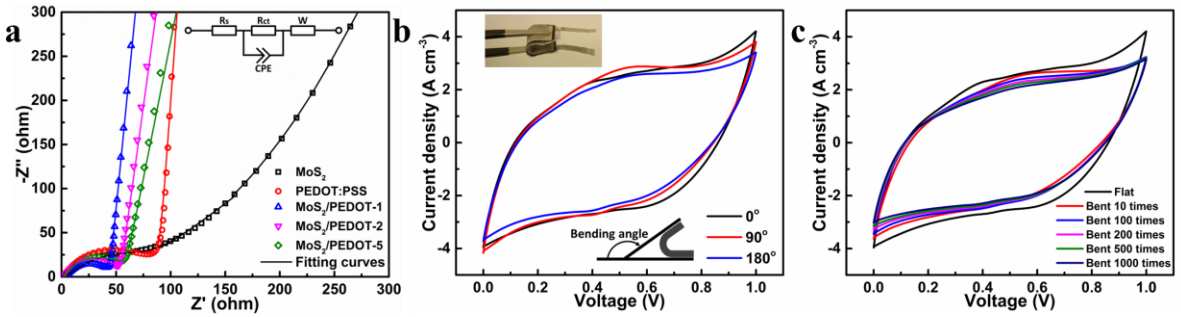

Table 1 Mechanical properties and electrical conductivities of MoS_2, PEDOT:PSS and MoS_2/PEDOT hybrid films.

Types of Films	Fracture strength (MPa)	Young's modulus (GPa)	Max elongation (%)	Conductivity (S cm^{-1})
PEDOT:PSS	35.9	1.3	3.8	104.2
MoS_2	5.3	2.7	0.3	0.5
MoS_2/PEDOT-1	23.5	1.9	1.4	17.9
MoS_2/PEDOT-2	18.0	2.0	0.9	11.9
MoS_2/PEDOT-5	7.4	2.2	0.4	4.4

Supporting information

A robust free-standing MoS_2/poly(3,4-ethylenedioxythiophene):poly(styrenesulfonate) film for supercapacitor applications

Yu Ge, Rouhollah Jalili, Caiyun Wang*, Tian Zheng, Yunfeng Chao and Gordon G. Wallace*

Intelligent Polymer Research Institute, ARC Centre of Excellence for Electromaterials Science, AIIM Facility, Innovation Campus, University of Wollongong, Wollongong, NSW 2522 Australia.

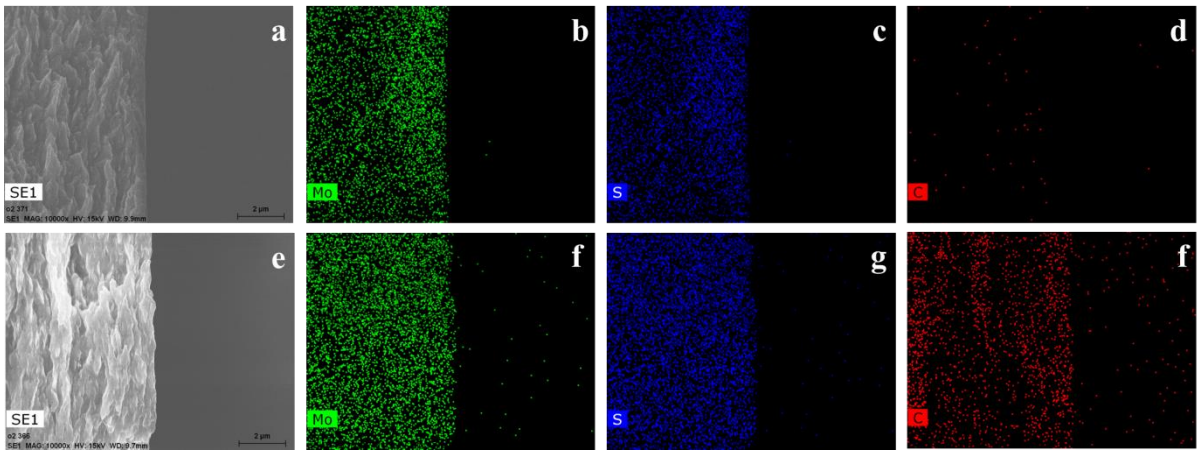

Figure S1 EDS mapping of Mo, S and C elements of the cross-section of MoS_2 (a-d) and MoS_2/PEDOT-2 films (e-f).

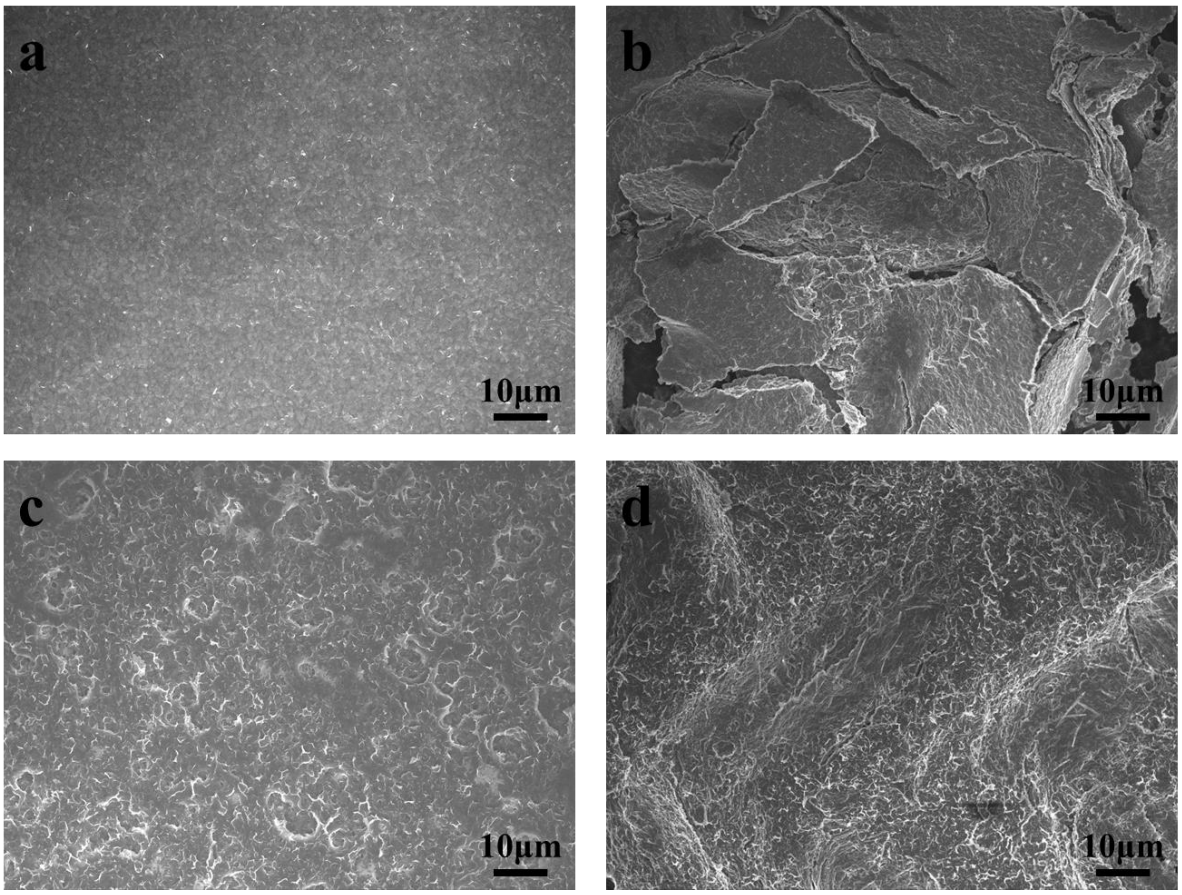

Figure S2 SEM images of MoS_2 (a, b) and MoS_2/PEDOT-2 films (c, d) before (a, c) and after (b, d) cycling test.

Table 1 R_s, R_{ct}, CPE-T and CPE-P values of the films.

Sample	R_s	R_s error	R_{ct}	R_{ct} error	CPE-T	CPE-T error	CPE-P	CPE-P error
MoS_2	2.64	0.12	106.7	4.8	3.7E-04	4.3E-05	0.638	0.014
PEDOT:PSS	1.58	0.08	90.6	4.4	1.9E-04	2.5E-05	0.747	0.015
MoS_2/PEDOT-1	2.46	0.09	50.6	2.7	6.0E-04	7.5E-05	0.632	0.015
MoS_2/PEDOT-2	1.95	0.08	57.8	3.6	5.0E-04	5.9E-05	0.663	0.014
MoS_2/PEDOT-5	1.89	0.07	69.5	4.2	4.9E-04	5.3E-05	0.674	0.013